SAND--96-2036C SAND 96-2036C
CONF-970231--27

A Near-Field Optical Microscopy Nanoarray

David J. Semin[a], W. Patrick Ambrose[a], Peter M. Goodwin[a],
Joel R. Wendt[b], and Richard A. Keller[a]

[a]Los Alamos National Laboratory
CST-1, MS M888
Los Alamos, NM 87545

[b]Sandia National Laboratories
Compound Semiconductor Technology
Dept. 1314, MS 0603
P.O. Box 5800
Albuquerque, NM 87185-0603

ABSTRACT

Multiplexing near-field scanning optical microscopy (NSOM) by the use of a nanoarray with parallel imaging is studied. The fabrication, characterization, and utilization of nanoarrays with ~ 100 nm diameter apertures spaced 500 nm center-to-center is presented. Extremely uniform nanoarrays with ~ 10^8 apertures were fabricated by electron beam lithography and reactive ion etching. The nanoarrays were characterized by atomic force microscopy (AFM) and scanning electron microscopy (SEM). In this paper we utilize these nanoarrays in a laser-illuminated microscope with parallel detection on a charge-coupled device (CCD). Detection of B-phycoerythrin (B-PE) molecules using near-field illumination is presented. In principle, our system can be used to obtain high lateral resolution NSOM images over a wide-field of view (e.g. 50-100 μm) within seconds.

Keywords: near-field scanning optical microscopy (NSOM), nanoarray, lithography, microscopy, fluorescence, imaging, charge transfer devices, single molecule detection

2. INTRODUCTION

In conventional near-field scanning optical microscopy (NSOM), a sub-wavelength aperture, such as a metal-coated tapered optical fiber, is used to illuminate a ~ 100 nm diameter area on a surface[1-5]. The aperture size defines the achievable lateral resolution. Lateral resolution on the order of 12 nm has been reported[4,5]. A NSOM fluorescence image is created point by point by raster scanning the aperture over a surface, or by raster scanning a surface under the aperture, the latter being more common. The advantage and popularity of NSOM arises from being able to create high resolution, spectrally resolved fluorescence images[6]. In addition, the detection of single molecules[5-7] using NSOM opens up new and exciting bioanalytical applications. Because NSOM and other scanned probe microscopy techniques (i.e. atomic force or scanning tunneling microscopies) rely on serial detection, they are limited to the imaging of essentially static systems. For imaging dynamic processes other techniques must be utilized. Although conventional (diffraction limited) optical microscopies can be used for imaging dynamic processes[8-13], these techniques lack the lateral resolution that can be obtained with NSOM.

In order to overcome the limitation of serial detection, while maintaining high lateral resolution, we have fabricated an array of near-field sources. By multiplexing the detection onto a charge-coupled device (CCD) much faster imaging rates can be obtained. An aluminum near-field nanoarray with ~ 100 nm diameter apertures spaced 500 nm center-to-center has

Further author information -
D.J.S.: Email: semin@lanl.gov; Telephone: 505-665-2092; Fax: 505-665-3024
W.P.A.: Email: wpa@lanl.gov; Telephone: 505-665-2092; Fax: 505-665-3024
P.M.G.: Email: pmg@lanl.gov; Telephone: 505-665-2092; Fax: 505-665-3024
J.R.W.: Email: jrwendt@sandia.gov; Telephone: 505-844-2649; Fax: 505-844-8985
R.A.K.(correspondence): Email: keller@lanl.gov; Telephone: 505-667-3018; Fax: 505-665-3024

DISCLAIMER

been fabricated by electron beam lithography and reactive ion etching. Extremely uniform nanoarrays with ~ 10^8 apertures were obtained. These arrays provide a means of maintaining high spatial resolution with parallel imaging to create near-field images. Each sub-wavelength aperture is imaged to a group of pixels on the CCD camera.

Historically, to make near-field light sources optical fiber probes[1-7], micropipettes[14,15], and individual isolated apertures in opaque metal films[16,17] were used. More recently, Pantano and Walt[18] have developed a system that uses a fiber bundle to create an array of near-field sources. To our knowledge, our system for multiplexing NSOM is the first reported use of a highly ordered nanoarray in an opaque metal film.

In this paper, we first present our wide-field laser-illuminated microscope that has the sensitivity to detect the locations of single fluorescent molecules. Using far-field Koehler epi-illumination[19] the detection of single molecules of Rhodamine 6G (R6G) on silica is demonstrated. Within seconds the locations of those single molecules within a ~ 56 x 56 μm^2 area is obtained. After presenting single molecule detection data using far-field epi-illumination, we then present the parallel, high resolution, detection of B-phycoerythrin (B-PE) molecules using near-field illumination from a nanoarray. B-PE is a highly fluorescent phycobiliprotein that is equivalent to ~ 20 R6G chromophores[20]. Using ~ 100 nm diameter apertures, the near-field illumination of B-PE molecules within a ~ 31 x 31 μm^2 area is demonstrated.

3. EXPERIMENTAL DETAILS

3.1 Microscope

Figure 1 is a schematic diagram for our parallel imaging NSOM instrument. Laser light from either a continuous-wave argon ion laser (514.5 nm, American Laser Corp.) or the second harmonic of a mode-locked Nd:YAG laser (532 nm, Quantronix) was passed through a line filter (LF) and sent into a multi-mode optical fiber (MMOF) via a fiber coupler (FC1). The MMOF was mechanically vibrated in order to scramble the phase and polarization of the laser beam[21,22]. After exiting the MMOF via a second fiber coupler (FC2), the light was split into two paths by use of a 50/50 beamsplitter (BS1; CVI Corp.). For focusing purposes and single molecule detection sensitivity experiments, one light path was directed into the epi-illumination port of the microscope by a 6.3 cm focal length lens (L1). The combination of the MMOF and Koehler illumination provides uniform illumination over a wide-field of view. The second light path was directed and focused at the near-field nanoarray by a 10 cm focal length lens (L2). Using this arrangement the incident irradiance was typically 1-5 W/cm^2. With appropriate beam blocks only one or the other path is used at any time. The fluorescence was collected with a high numerical aperture (NA) microscope objective: either a 100x, 1.1 NA oil-immersion objective (Carl Zeiss Inc.); or a 60x, 1.2 NA water-immersion objective (Nikon Corp.). A dichroic beamsplitter (BS2; Omega Optical) and Raman edge filter (RF; Omega Optical) were used to reject scattered light. Fluorescence light collected from the microscope objective was then imaged at the first lens of the relay lens assembly (RLA, HRX250-NIK; Diagnostic Instruments). The RLA is used to magnify the image ~ 2.5x onto a liquid nitrogen-cooled CCD camera (Princeton Instruments). The CCD camera was equipped with a 512 x 512 back-illuminated array format and was operated at 50 KHz using a ST-138 controller (Princeton Instruments) coupled to a computer (OptiPlex XMT 5120; Dell Inc.).

3.2 R6G Deposition

R6G (R590 chloride, Exciton) was dissolved in methanol and diluted to approximately 10^{-10} M. This sample was then spin-coated onto 160 μm thick fused silica cover slips (ESCO Products, Inc.).

3.3 Nanoarray Fabrication

The aluminum nanoarrays were fabricated on fused silica cover slips (ESCO Products, Inc.). The cover slips were cleaned with Chromerge acid (Sigma-Aldrich Corp.), followed by exhaustive sonication in methanol and finally water. The cover slips were then dried with flowing nitrogen gas. The cleaned cover slips were placed into a vacuum chamber and argon ion milled for 45 seconds, following which 120 nm of aluminum was electron-beam deposited. The argon ion milling step was necessary to improve adhesion of the aluminum to the fused silica. Next, a 420 nm thick polymethylmethacrylate (PMMA) film was deposited on the aluminum coated cover slip by spin coating a 6 % PMMA solution at 5500 rpm for 30 seconds. The cover slip was then baked at 170 °C for two hours. A JEOL JBX-5FE electron beam lithography system with a thermal field emission gun was then used to expose the PMMA. The electron beam writing step formed a square lattice array with spots ~ 100 nm in diameter spaced 500 nm center-to-center. Next, a reactive ion etching step using BCl_3/Cl_2 was used to etch away the aluminum from the exposed holes. Typical etching times were 6-8 minutes. Finally, an oxygen etching step was utilized to remove the remaining PMMA from the aluminum substrate. Using this procedure, ~ 10^8 apertures 100 nm in diameter and spaced 500 nm center-to-center were fabricated in a 4.8 x 4.8 mm^2 area on a fused silica cover slip.

3.4 B-PE Near-field Illumination

B-PE (Molecular Probes) was dissolved in 1x Dulbecco's phosphate-buffered saline (DPBS, Gibco BRL) and diluted to approximately 10^{-8} M. For imaging, approximately 10 μl of the dilute B-PE sample was placed onto a nanoarray.

4. RESULTS AND DISCUSSION

4.1 Single Molecule Detection Sensitivity with Epi-illumination

Using the optical arrangement as shown in Figure 1 with unpolarized 514.5 nm excitation and a 6.3 cm focal length lens (L1 in Fig. 1) for Koehler epi-illumination, a wide-field image was obtained. For uniform illumination across the field of view, the MMOF scrambling is essential[21,22]. For our experimental setup the illumination deviation over a 56 x 56 μm^2 area was less than 10 %. Figure 2 shows representative wide-field, epi-illumination, fluorescence images of single R6G molecules on fused silica. R6G has maximum absorption and emission at 528 and 551 nm, respectively[23]. The top image in Figure 2 is 56 x 56 μm^2 in size with an exposure time of 5 seconds. The bright spots represent the locations of single R6G molecules. The spatial resolution is diffraction limited (i.e. spot diameter ~ 400 nm). The bottom image in Figure 2 is a surface plot of fluorescence intensity versus lateral position taken from the boxed area of the top image. A characteristic trait of single molecules is the abrupt photobleaching that occurs[7,24-27]. Photobleaching is the irreversible loss of fluorescence. Whereas, for an ensemble of molecules gradual fading of the fluorescence signal is observed. In our case, single R6G molecules display fluorescence intensity fluctuations (data not shown) and then bleach abruptly during continuous irradiation[7]. To explain the fluorescence intensity fluctuations it is postulated that changes in the local environment of the molecule, or the molecule itself, may be affecting the photophysical parameters (e.g. lifetime) of the molecules. We have studied numerous other xanthene dyes that exhibit this unexpected and unusual behavior (e.g. fluorescein, tetramethylrhodamine-isothiocyanate, tetramethylrhodamine-5-isothiocyanate, and rhodamine B).

Although wide-field epi-illumination microscopes can be used to track the diffusion of fluorescent particles, often higher lateral resolution is desired. Based on using a Gaussian function to fit a fluorescence intensity profile, many groups[8-13] have reported positional accuracies well below the optical diffraction limit. With the use of a nanoarray with parallel imaging, the positional accuracy is ultimately determined by the aperture diameter and not by Gaussian fitting of intensity profiles. For an object to be excited efficiently it must be within the near-field region of the aperture. The near-field region extends outward a distance on the order of the diameter of the aperture. With the use of high NA microscope objectives, which have small depth-of-focus, fluorescence from objects outside the near-field region is not imaged. The advantage of our system is in improved resolution with parallel detection. Characterization of the morphology and transmission efficiency of the nanoarrays is described below.

4.2 Nanoarray Morphology

Atomic force microscopy (AFM) and scanning electron microscopy (SEM) were used to characterize the array. Contact-mode atomic force micrographs were taken with a Nanoscope III (Digital Instruments) using an etched single-crystal Si probe at a scan rate of 1 Hz. Representative AFM images are shown in Figure 3. The array pattern is very uniform with apertures (dark regions) ~ 100 nm in diameter and spaced 500 nm center-to-center. The reactive ion etching times can be used to control the aperture diameters. For instance, the top micrograph in Figure 3 shows a nanoarray sample that was etched for 7 minutes. The bottom micrograph in Figure 3 was a sample that was etched for 8 minutes. The AFM provides information about the top of the array, but does not measure the bottom of the holes due to the convolution problem of the AFM tip with the inside wall of the apertures. For the top of the apertures AFM analysis indicated an approximate diameter dimension of 150 and 200 nm for the 7 and 8 minute etch samples, respectively. AFM analyses on multiple regions with multiple probes was used to verify the uniformity and morphology of the nanoarrays. A SEM was used to assess the aperture morphology in the bottom of the holes. Using SEM, it was found that at the bottom (i.e. aluminum/quartz interface of the aperture) the approximate diameter was 70 and 100 nm for the 7 and 8 minute etch samples, respectively. A tapered hole results from mask erosion during etching. Having measured the morphology, we proceeded to measure the corresponding transmission efficiency.

4.3 Transmission Efficiency

Elegant work on understanding tapered near-field probe transmission efficiencies was carried out by Valaskovic et al.[28] They and others[29,30] have shown that tapered NSOM fiber probe transmission efficiencies are on the order of 10^{-4} to 10^{-8} (typically nW far-field output with mW input power). As reported by Valaskovic et al., the transmission efficiency of an optical fiber probe is critically dependent on the taper shape and morphology of the aluminum coating at the end of the fiber.

To determine the transmission efficiency of the nanoarrays the dichroic beamsplitter (BS2) and Raman edge filter (RF) were removed from the optical path. As shown in Figure 1, the unpolarized laser light (514.5 nm) was focused onto the near-field nanoarray by L2. A comparison was made between light focused onto a fused silica cover slip and light focused onto the nanoarray. Figure 4 shows the arrangement for this measurement. Note in Figure 4B the schematic showing the approximate shape of the apertures. The same incident irradiance and integration time were used for the two measurements.

Interestingly, the transmission efficiencies for the 7 and 8 minute reactive ion etch samples were 1×10^{-2} and 5×10^{-2} (ratio of CCD camera integrated counts for nanoarray:fused silica), respectively. These transmission efficiencies are within a factor of two of the calculated geometric efficiencies using the aperture bottom diameters obtained from SEM measurements. For aperture diameters below the diffraction limit ($< \lambda/2$), one expects the transmission of a single aperture to be less than the geometrical value. It was surprising to find that this combination of taper shape and center-to-center aperture distance produce highly transmissive devices. This result may arise from affects similar to cooperative emission from a phased array of radiating dipoles.

Always a concern with using a NSOM fiber optic probe is the localized heating[31] of the tip due to the high attenuation for a tapered metal-coated sub-wavelength aperture[28]. Localized heating of the sample surface can result from the close proximity of a metal-coated optical fiber to the surface. Additionally, depending on the brightness of the sample, one often needs to make a compromise between the desired light flux and aperture diameter of a fiber optic probe. This compromise typically forces one to image slower and with a lower resolution in order to obtain a reasonable signal-to-noise ratio. Hence, one possible advantage of our light-efficient nanoarrays is that less sample heating is expected.

4.4 B-PE Near-field Illumination

In order to investigate near-field illumination using these nanoarrays, a 10^{-8} M B-PE solution was placed on the 8 minute etch nanoarray and a cover slip was placed on top. Using the configuration in Figure 1 with 532 nm excitation and a 100x, 1.1 NA microscope objective, the fluorescence from the B-PE was collected and imaged. B-PE has maximum absorption and emission at 540 and 575 nm, respectively[23]. A representative image of B-PE molecules on the nanoarray is shown in Figure 5. The image integration time was 10 seconds. The array pattern is evident, with different brightnesses arising from each aperture. A sequence of such images reveals many static features, occasional brightening in some holes, abrupt disappearance of signal from one frame to the next, and an eventual overall dimming (due to bleaching). An estimate for the signal from a single B-PE is approximately equal to the signal integrated over the brightest spots (1300 photoelectrons/sec with an average irradiance of ~ 1 W/cm2). We have observed that B-PE adheres well to silicon-oxide surfaces. Hence, we interpret the image in Fig. 5 as follows. The B-PE in the solution diffuse until they encounter and stick to the oxide surfaces of the array (silicon and aluminum oxides). With an initial concentration of 10^{-8} M in the liquid, an approximate liquid layer thickness of 10 micrometers, and an open area in the metal film of 3 %, approximately 1/2 of the holes would be occupied by a single B-PE. The brightest spots are from single B-PE near the middle of the aperture away from the metal. The distribution of brightnesses arise from B-PE fixed at random locations within the metal structure, which produces different excitation and quenching rates (quenching by proximity to the metal). This example shows the feasibility of multiplexing NSOM by using an array of apertures and parallel far-field imaging over a wide-field of view.

5. CONCLUSIONS

We have explored the preparation and properties of an array of near-field sources. Uniform arrays of nano-scale holes were produced in an opaque metal film on a transparent glass substrate, and characterized using SFM and SEM. We have demonstrated single molecule detection by fluorescence excitation and quick imaging using parallel optical detection in a cooled CCD camera. Experiments and calculations aimed at understanding the intriguingly high transitivity of the nanoarrays are in progress.

ACKNOWLEDGMENT

D.J.S. wishes to thank the Director's Office at Los Alamos National Laboratory (LANL) for a Director's Funded Postdoctoral Fellowship. The authors wish to thank Sally Samora at Sandia National Laboratories for help in preparing the nanoarray samples. D.J.S. wishes to thank Marilyn Hawley and Robert Cary at LANL for the use of their atomic force microscopes, and Harvey L. Nutter at LANL for technical assistance. A portion of this work was supported by the United States Department of Energy under Contract DE-AC04-94AL85000. Sandia is a multiprogram laboratory operated by Sandia Corporation, a Lockheed Martin Company, for the United States Department of Energy.

REFERENCES

1. U. Dürig, D.W. Pohl, and F. Rohner, "Near-Field Optical-Scanning Microscopy", *J. Appl. Phys.* **59** pp. 3318-3327, 1986.
2. D.W. Pohl (Eds. C.J.R. Sheppard and T. Mulvey), in *Advances in Optical and Electron Microscopy*, "Scanning Near-Field Optical Microscopy (SNOM)", pp. 243-312, Academic Press, New York, 1991.

3. E. Betzig, J.K. Trautman, T.D. Harris, J.S. Weiner, and R.L. Kostelak, "Breaking the Diffraction Barrier: Optical Microscopy on a Nanometric Scale", *Science* **251** pp. 1468-1470, 1991.
4. E. Betzig and J.K. Trautman, "Near-Field Optics: Microscopy, Spectroscopy, and Surface Modification Beyond the Diffraction Limit", *Science* **257** pp. 189-195, 1992.
5. E. Betzig and R.J. Chichester, "Single Molecules Observed by Near-Field Scanning Optical Microscopy", *Science* **262** pp. 1422-1425, 1993.
6. J.K. Trautman, J.J. Macklin, L.E. Brus, and E. Betzig, "Near-Field Spectroscopy of Single Molecules at Room-Temperature", *Nature* **369** pp. 40-42, 1994.
7. W.P. Ambrose, P.M. Goodwin, J.C. Martin, and R.A. Keller, "Single Molecule Detection and Photochemistry on a Surface Using Near-Field Optical Excitation", *Phys. Rev. Lett.* **72** pp. 160-163, 1994.
8. Th. Schmidt, G.J. Schütz, W. Baumgartner, H.J. Gruber, and H. Schindler, "Characterization of Photophysics and Mobility of Single Molecules in a Fluid Lipid Membrane", *J. Phys. Chem.* **99** pp. 17662-17668, 1995.
9. Th. Schmidt, G.J. Schütz, W. Baumgartner, H.J. Gruber, and H. Schindler, "Imaging of Single Molecule Diffusion", *Proc. Natl. Acad. Sci.* **93** pp. 2926-2929, 1996.
10. R.M. Dickson, D.J. Norris, Y.L. Tzeng, and W.E. Moerner, "3-Dimensional Imaging of Single Molecules Solvated in Pores of Poly(Acrylamide) Gels", *Science* **274** pp. 966-969, 1996.
11. H.P. Kau and A.S. Verkman, "Tracking of Single Fluorescent Particles in Three Dimensions: Use of Cylindrical Optics to Encode Particle Position", *Biophys. J.* **67** pp. 1291-1300, 1994.
12. I.E.G. Morrison, C.M. Anderson, G.N. Georgiou, G.V.W. Stevenson, and R.J. Cherry, "Analysis of Receptor Clustering on Cell Surfaces by Imaging Fluorescent Particles", *Biophys. J.* **67** pp. 1280-1290, 1994.
13. C.M. Anderson, G.N. Georgiou, I.E.G. Morrison, G.V.W. Stevenson, and R.J. Cherry, "Tracking of Cell Surface Receptors by Fluorescence Digital Imaging Microscopy using a Charge-Coupled Device Camera", *J. Cell Sci.* **101** pp. 415-425, 1992.
14. K. Lieberman and A. Lewis, "Simultaneous Scanning Tunneling and Optical Near-Field Imaging with a Micropipette", *Appl. Phys. Lett.* **62** pp. 1335-1337, 1993.
15. S. Shalom, K. Lieberman, A. Lewis, and S.R. Cohen, "A Micropipette Force Probe suitable for Near-Field Scanning Optical Microscopy", *Rev. Sci. Instr.* **63** pp. 4061-4065, 1992.
16. U.Ch. Fischer, "Submicrometer Aperture in a Thin Metal Film as a Probe of its Microenvironment through Enhanced Light Scattering and Fluorescence", *J. Opt. Soc. Am. B. Opt. Phys* **3** pp. 1239-1244, 1986
17. U.Ch. Fischer, "Optical Characteristics of 0.1 um Circular Apertures in a Metal Film as Light Sources for Scanning Ultramicroscopy", *J. Vac. Sci. Technol. B.* **3** pp. 386-390, 1985
18. P. Pantano and D.R. Walt, "Near-Field Optical Arrays", In press, *Rev. Sci. Instr.*
19. D.M. Pallister and M.D. Morris, "Laser Koehler Epi-Illumination for Raman and Fluorescence Microscopic Imaging", *Appl. Spec.* **48** pp. 1277-1281, 1994.
20. M. Wu, P.M. Goodwin, W.P. Ambrose, and R.A. Keller, "Photochemistry and Fluorescence Emission Dynamics of Single Molecules in Solution: B-Phycoerythrin", *J. Phys. Chem.* **100** pp. 17406-17409, 1996.
21. R. Hard, R. Zeh and R.D. Allen, "Phase-Randomized Laser Illumination for Microscopy", *J. Cell Sci.* **23** pp. 335-343, 1977.
22. G.W. Ellis, "A Fiber-optic Phase-Randomizer for Microscope Illumination by Laser", *J. Cell Biol.* **83** pp. 303a, 1979.
23. Moleculer Probes, "Handbook of Fluorescent Probes and Research Chemicals", by Richard P. Haugland, 6th Edition.
24. W.P. Ambrose, P.M. Goodwin, J.C. Martin, and R.A. Keller, "Alterations of Single Molecule Fluorescence Lifetimes in Near-Field Optical Microscopy", *Science* **265** pp. 364-367, 1994.
25. W.P. Ambrose, R.L. Affleck, P.M. Goodwin, R.A. Keller, J.C. Martin, J.T. Petty, J.A. Schecker, M. Wu, "Imaging Biological Molecules with Single Molecule Sensitivity using Near-Field Scanning Optical Microscopy", *Exp. Tech. Phys.* **41** pp. 237-248, 1995.
26. X.S. Xie and R.C. Dunn, "Probing Single-Molecule Dynamics", *Science.* **265** pp. 361-364, 1994.
27. A.J. Meixner, D. Zeisel, M.A. Bopp and G. Tarrach, "Superresolution Imaging and Detection of Fluorescence from Single Molecules by Scanning Near-Field Optical Microscopy", *Opt. Eng.* **34** pp. 2324-2332, 1995.
28. G.A. Valaskovic, M. Holten and G.H. Morrison, "Parameter Control, Characterization, and Optimization in the Fabrication of Optical Fiber Near-Field Probes", *Appl. Opt.* **34** pp. 1215-1228, 1995.
29. E. Betzig, R.J. Chichester, F. Lanni and D.L. Taylor, "Near-field Fluorescence Imaging of Cytoskeletal Actin", *Bioimaging.* **1** pp. 129-135, 1993.
30. R.C. Dunn, G.R. Holtom, L. Mets and X.S. Xie, "Near-field Fluorescence Imaging and Fluorescence Lifetime Measurement of Light Harvesting Complexes in intact Photosynthetic Membranes", *J. Phys. Chem.* **98** pp. 3094-3098, 1994.
31. M. Stahelin, M.A. Bopp, G. Tarrach, A.J. Meixner, and I. Zschokkegranacher, "Temperature Profile of Fiber Tips used in Scanning Near-field Optical Microscopy", *Appl. Phys. Lett.* **68** pp. 2603-2605, 1996.

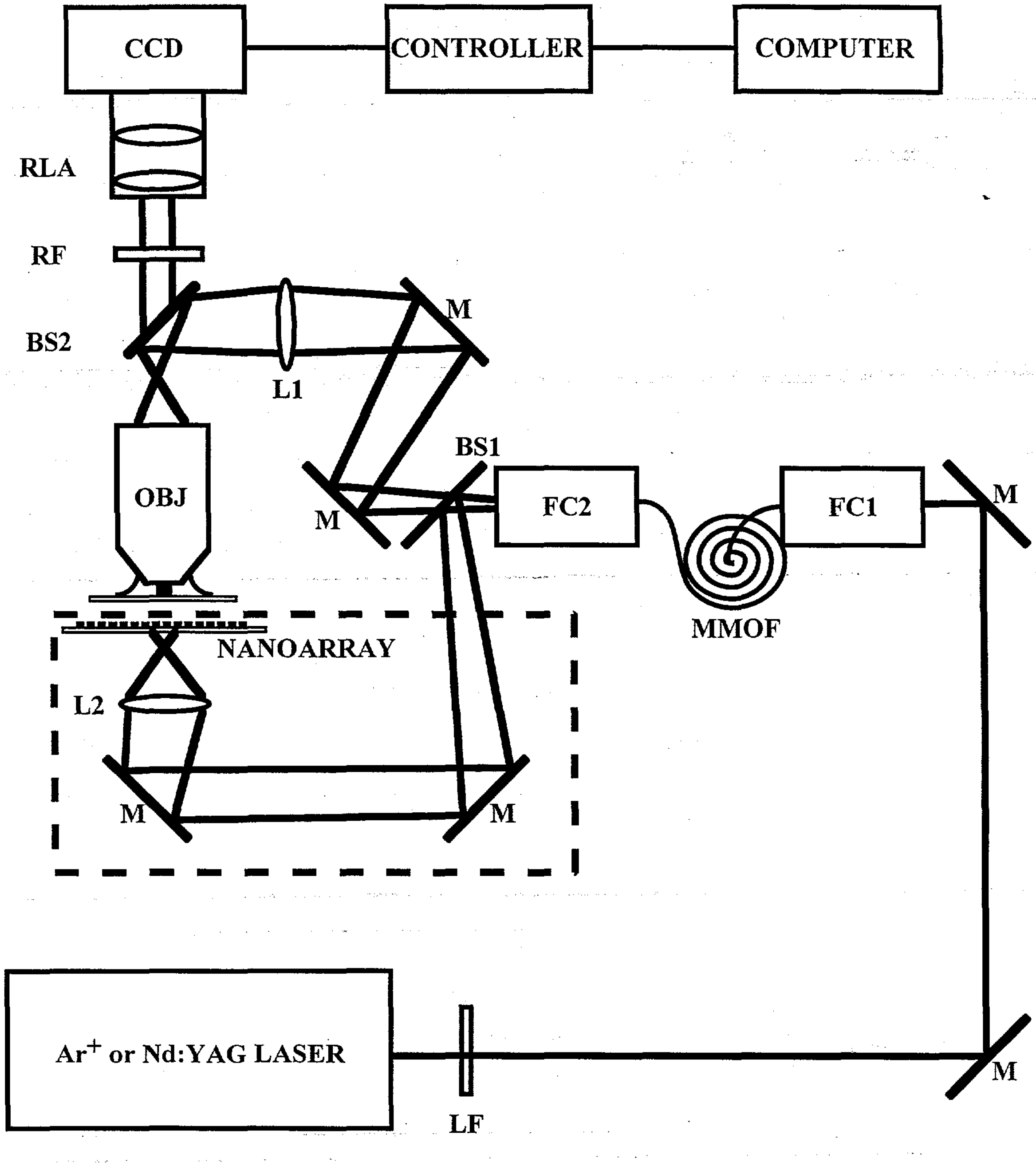

Figure 1: Schematic of laser-illuminated parallel imaging microscope. See text for details.

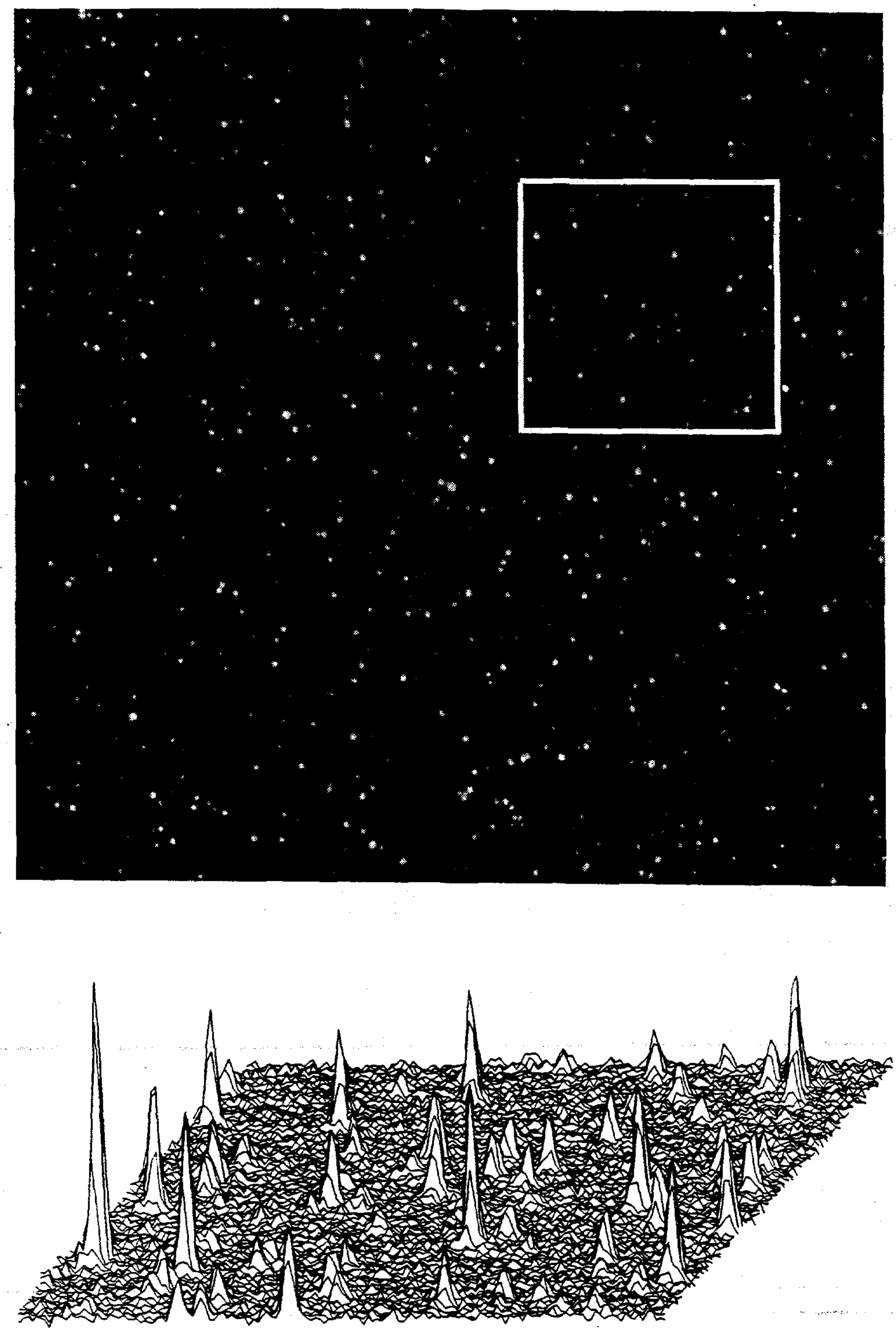

Figure 2: Fluorescence image showing the locations of single R6G molecules on a fused silica cover slip. The top picture represents a 56 x 56 μm^2 region. The bottom picture is a surface plot taken from the boxed region of the top picture. The total integration time was 5 seconds. A 60x, 1.2 NA water-immersion microscope objective was used for excitation and collection.

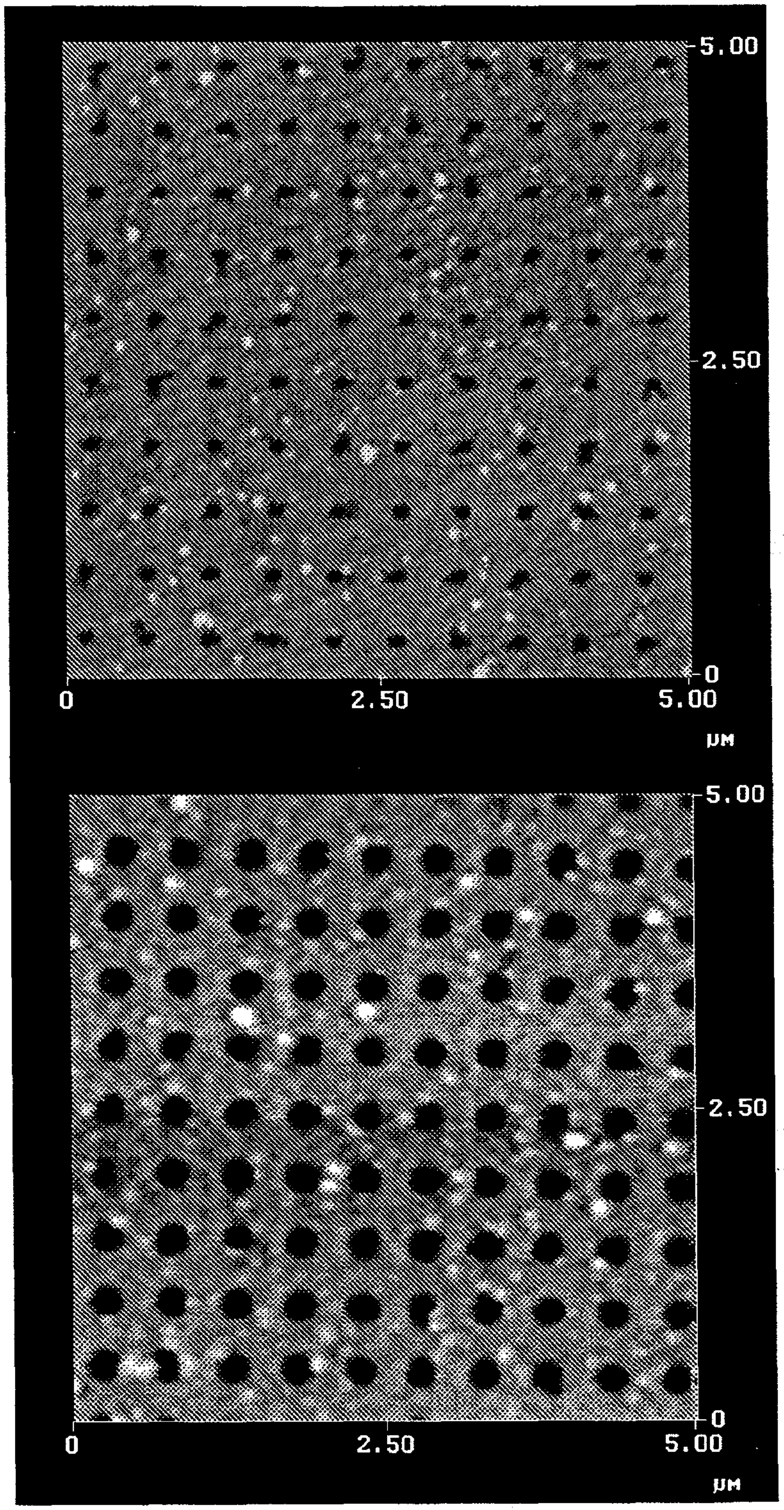

Figure 3: Representative atomic force micrographs of an electron beam fabricated nanoarray. The array consists of holes in a thin aluminum film on silica. The top micrograph represents a sample that had a 7 minute reactive ion etching step. The bottom micrograph represents a sample that had an 8 minute reactive ion etching step.

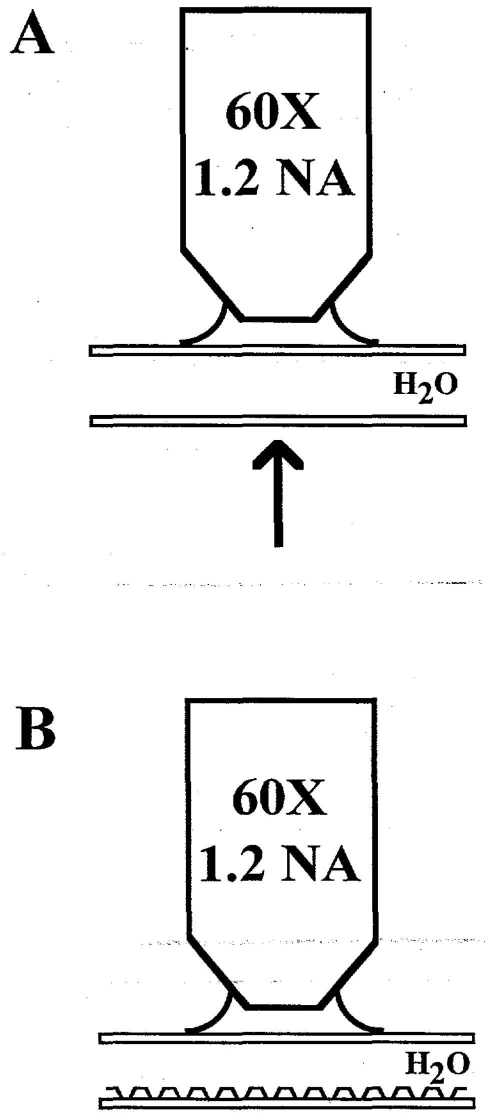

Figure 4: Array transmission efficiency measurement. Panels A and B represent the arrangements for the transmission measurements for a fused silica reference and the nanoarrays, respectively. A 60x, 1.2 NA water-immersion microscope objective was used for collection. The arrow represents the direction of the laser beam.

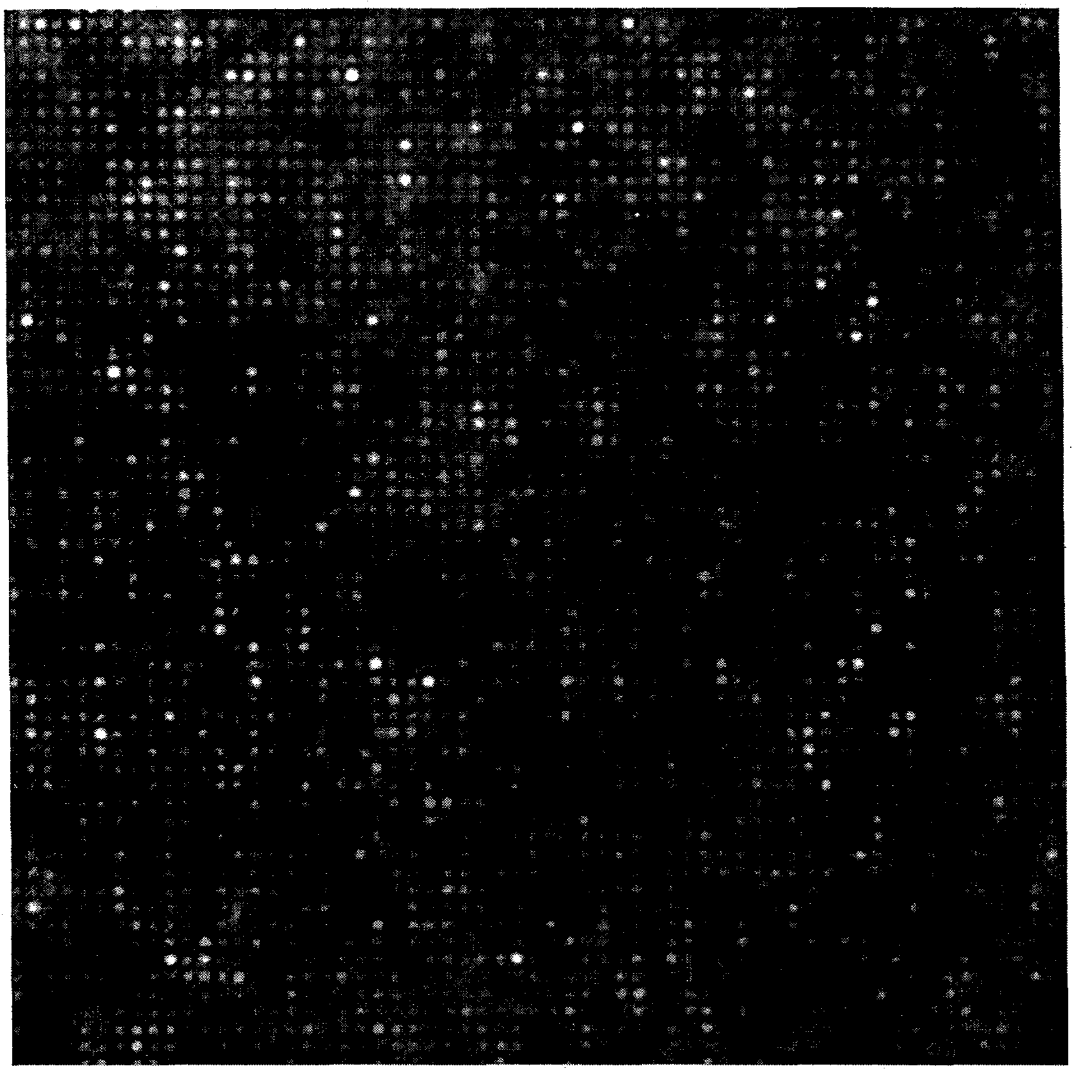

Figure 5. Fluorescence image of B-PE molecules illuminated through a nanoarray. The image is 31 x 31 μm^2 in size. See text for details.